

Is the silicate emission feature only influenced by grain size?

N.V. Voshchinnikov^{1,2} and Th. Henning³

¹ Sobolev Astronomical Institute, St. Petersburg University, Universitetskii prosp. 28, St. Petersburg, 198504 Russia, e-mail: nvv@astro.spbu.ru

² Isaac Newton Institute of Chile, St. Petersburg Branch

³ Max-Planck-Institut für Astronomie, Königstuhl 17, D-69117 Heidelberg, Germany

Received March 3, 2008 / accepted March 21, 2008

Abstract. The flattening of the 10 μm silicate emission feature observed in the spectra of T Tauri and Herbig Ae/Be stars is usually interpreted as an indicator of grain growth. We show in this paper that a similar behaviour of the feature shape occurs when the porosity of composite grains varies. The fluffy aggregates, having inclusions of different sizes, were modeled by multi-layered spheres consisting of amorphous carbon, amorphous silicate and vacuum. It is also found that the inclusion of crystalline silicates in composite porous particles can lead to a shift of the known resonances and production of new ones.

1. Introduction

The shape and strength of the silicate emission feature observed near 10 μm in the spectra of T Tauri and Herbig Ae/Be (HAeBe) stars is commonly used as a measure of grain growth in protoplanetary discs (see Natta et al. 2007 for a review). It is well known theoretically that with an increase of the grain size, the feature becomes wider and eventually fades away. In the case of compact spherical grains with composition of astronomical silicate, the 10 μm feature disappears when the grain radius exceeds $\sim 2 \mu\text{m}$ (see Fig. 1).

The standard approach to modelling of the 10 μm feature includes calculations of light absorption by several populations of compact (and hollow) silicate spheres. Amorphous and crystalline particles of small and large sizes are used to fit the observed emission profiles. The model was first suggested by Bouwman et al. (2001) and then modified by van Boekel et al. (2005). It was used by Schegerer et al. (2006), Honda et al. (2006), Kessler-Silacci et al. (2006), Sargent et al. (2006), Sicilia-Aguilar et al. (2007), Bouwman et al. (2008) to fit the observational data. Further the authors searched for correlations between the estimated mass fractions of large and crystalline grains and different stellar and disc parameters like mass, luminosity, age, spectral type, etc. As a rule, the correlations are absent or rather weak (see Table 5 in the paper of Sicilia-Aguilar et al., 2007).

In this Letter we show that the shape, position and strength of the 10 μm silicate feature is also influenced by variations of the properties of small mass composite aggregate grains. The fluffy aggregates were modeled by multi-layered spheres (see also Voshchinnikov et al., 2006). This particle model permits us to include an arbitrary fraction of materials, and computations do not require large resources.

2. Model of porous composite grains

Fluffy particles should appear as a result of grain coagulation in interstellar clouds and protoplanetary discs (e.g., Henning & Stognienko, 1996; Dominik & Tielens, 1997; Jones, 2004; Ormel et al., 2007). It is expected that aggregates can consist of several silicate and carbon sub-particles of different sizes which can be treated as inclusions in a vacuum matrix.

We use the model of spherical multi-layered particles introduced by Voshchinnikov & Mathis (1999). Later, Voshchinnikov et al. (2005) have demonstrated that the optical properties of layered spheres resemble those of fluffy aggregates having inclusions of different sizes.

Our model parameters are: the refractive indices and volume fractions V_i/V_{total} of the materials and the radius of compact particles r_{compact} . The amount of vacuum in the particle (the *particle porosity* \mathcal{P} , $0 \leq \mathcal{P} < 1$) is

$$\mathcal{P} = V_{\text{vac}}/V_{\text{total}} = 1 - V_{\text{solid}}/V_{\text{total}}, \quad (1)$$

where V_{solid} is the sum of the volumes of all species excluding vacuum. The radius of porous particles is related to that of compact particles as

$$r_{\text{porous}} = \frac{r_{\text{compact}}}{(1 - \mathcal{P})^{1/3}} = \frac{r_{\text{compact}}}{(V_{\text{solid}}/V_{\text{total}})^{1/3}}. \quad (2)$$

The model of layered spheres combines all components including vacuum in *one* particle (internal mixing) in contrast to the standard approach discussed above where “external mixing” (mixture of several individual populations of compact grains) is used.

For calculations, we use different kinds of carbon and silicates: amorphous carbon Be1 and AC1 (Rouleau & Martin, 1991), amorphous silicate with olivine composition (Dorschner et al., 1995), crystalline olivine (Fabian et al., 2001), and astronomical silicate (astrosil; Laor & Draine, 1993).

3. Analysis of silicate emission

The silicate feature in the N band was observed in spectra of a large variety of objects (see Henning 2008 for a recent review). We should caution the reader that we calculate absorption efficiencies, but measure the fluxes. A detailed analysis of disc spectra certainly requires radiative transfer calculations. Assuming that the silicate emission is optically thin we can compare observed fluxes with theoretical profiles. The latter are proportional to the product of particle absorption cross section by the Planck function with the particle temperature $\propto C_{\text{abs}}(\lambda) B_{\lambda}(T_d)$. Radiative transfer calculations show that grains of different temperatures contribute to the silicate feature (see Fig. 1 in Schegerer et al., 2006). However, the dominating contribution for the $10 \mu\text{m}$ feature comes from particles with $T_d = 200 - 400\text{K}$ for which the Planck function is approximately constant in N band. Therefore, we can adopt that the shape of the feature depends primarily on the emission properties of grains¹.

The profile of the feature can be described by the *normalized absorption efficiency factor* (and observationally by the normalized flux after the fitting and subtraction of continuum) $Q_{\text{abs}}(\lambda)/Q_{\text{abs}}(\lambda_0) - 1$, where the flux at wavelength λ_0 characterizes the continuum. As usual, the value of $\lambda_0 = 8.2 \mu\text{m}$ is chosen (e.g., Schegerer et al., 2006).

Another representation of the optical behaviour is provided by the *mass absorption coefficient* which is the ratio of absorption cross section $C_{\text{abs}}(\lambda)$ to particle mass. In the case of a sphere of porosity \mathcal{P} , it can be written as

$$\kappa_{\text{abs}}(\lambda) = \frac{C_{\text{abs}}(\lambda)}{\rho_d V_{\text{total}}} = \frac{3 Q_{\text{abs}}(\lambda)}{4 \rho_{d, \text{solid}} r_{s, \text{compact}} (1 - \mathcal{P})^2/3}, \quad (3)$$

where $\rho_d = \rho_{d, \text{solid}}(1 - \mathcal{P})$ is the mean particle density. The value of $\rho_{d, \text{solid}}$ is obtained by averaging the density of all species excluding vacuum. In our calculations we assume that $\rho_{d, \text{Si}} = 3.3 \text{ g/cm}^3$ and $\rho_{d, \text{C}} = 1.85 \text{ g/cm}^3$ for silicate and carbon, respectively.

Figure 1 shows the wavelength dependence of the normalized absorption efficiency factors for compact silicate spheres of diverse sizes. With a growth of the particle size (and mass) the $10 \mu\text{m}$ silicate feature broadens, its height decreases and the position of maximum shifts to longer wavelengths.

In a similar manner, the silicate feature changes when the particle porosity grows (Fig. 2). However, in this case the particle size increases only moderately, while particle mass remains the same. With a growth of porosity the peak strength decreases for normalized absorption (Fig. 2, upper panel) whereas the mass absorption coefficient becomes larger (Fig. 2, lower panel). The value of κ_{abs} almost doubles at the peak position when we replace the compact particle by porous particle.

It is well known that the shape and strength of the silicate feature depend on the type of the amorphous silicate, particle size and fractal dimension (see, e.g., van Boekel et al., 2005, Schegerer et al., 2006, Min et al., 2006). Using the model of

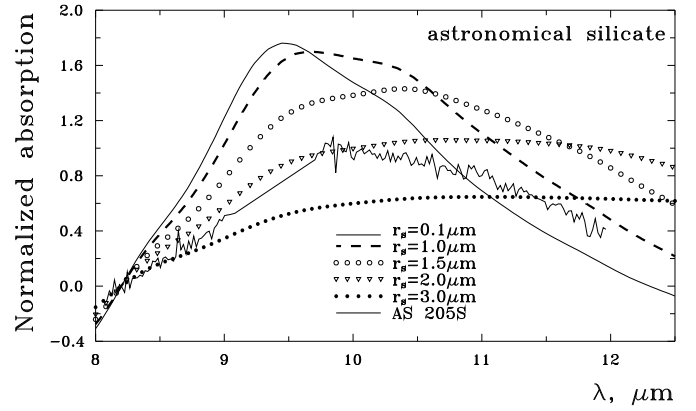


Fig. 1. Wavelength dependence of the normalized absorption efficiency factor $[Q_{\text{abs}}(\lambda)/Q_{\text{abs}}(8.2 \mu\text{m}) - 1]$ for compact spheres consisting of astrosil. The effect of variation of the silicate emission shape with the particle size is illustrated. The observational profile of the T Tauri star ‘AS 205S’ (Schegerer et al., 2006) is shown for comparison. Note that this profile is continuum subtracted.

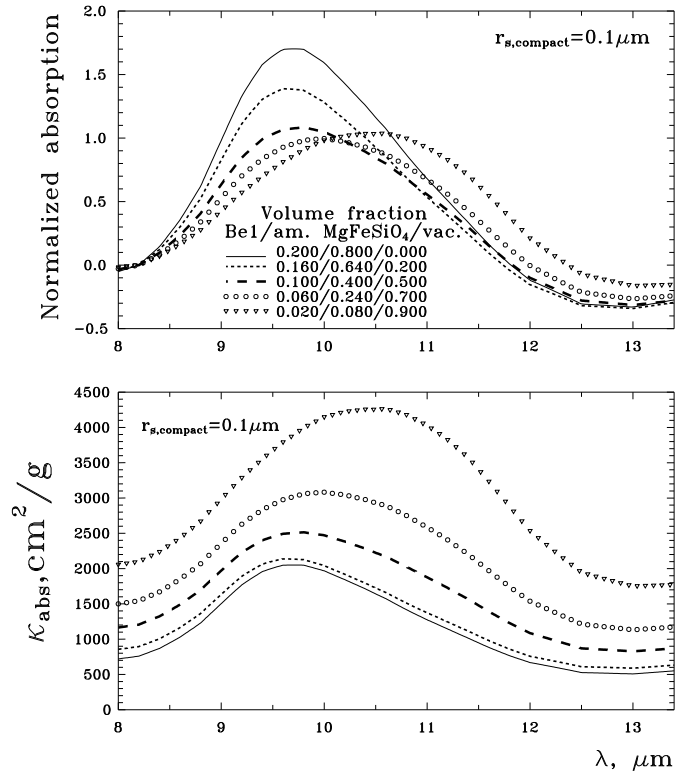


Fig. 2. Wavelength dependence of the normalized absorption efficiency factor (upper panel) and mass absorption coefficient (lower panel) for layered spheres with $r_{s, \text{compact}} = 0.1 \mu\text{m}$. The particles consist of amorphous carbon (Be1), amorphous silicate with olivine composition (MgFeSiO_4) and vacuum. The volume fraction of components V_i/V_{total} is indicated. The particles are of the same mass ($V_{\text{Be1}}/V_{\text{solid}} = V_{\text{Be1}}/(V_{\text{Be1}} + V_{\text{MgFeSiO}_4}) = 0.2$) but of different porosity. The solid curves correspond to compact particles. The effect of variation of the silicate emission shape with the particle porosity is illustrated.

¹ Note that our case differs from the case analyzed by Li et al. (2004) where the cometary particles of different composition are located at the same distance from the Sun.

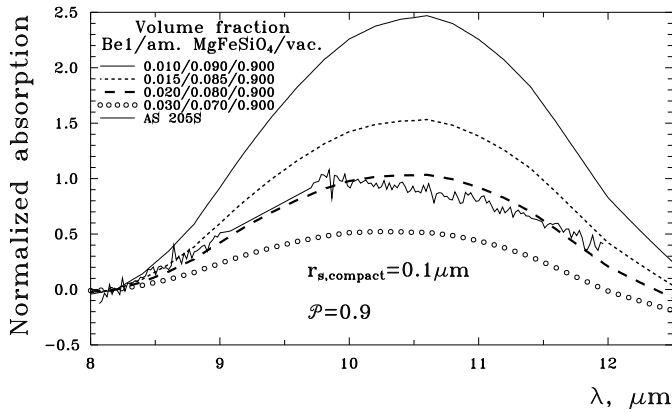


Fig. 3. The same as in Fig. 2 (upper panel) but now for particles of porosity $\mathcal{P} = 0.9$. The particles are of the same porosity but of slightly different mass. The value of $V_{\text{Be1}}/V_{\text{solid}}$ varies from 0.1 to 0.3. The effect of variation of the silicate emission shape with the volume fraction of carbon is illustrated. The observational profile of the T Tauri star AS 205S (Schegerer et al., 2006) is shown for comparison.

composite grains we can also investigate how carbon embedded in particles affects the characteristics of the silicate feature. This dependence is plotted in Fig. 3. With addition of carbon, the feature very rapidly transforms into a plateau and then disappears.

Comparing the data presented in Figs. 1 and 3 with observations, it is possible to estimate characteristics of grains fitting the observations: $r_{\text{s,compact}} \approx 2.0 \mu\text{m}$ or $V_{\text{Be1}}/V_{\text{solid}} \approx 0.2$ and $r_{\text{s,porous}} \approx 0.215 \mu\text{m}$ (last value is obtained from Eq. (2) for $\mathcal{P} = 0.9$). Hence the same observational data can be explained with particles whose radii differ by a factor of ~ 9 and masses by a factor of ~ 8800 (!).

Using the observations from Schegerer et al. (2006), van Boekel et al. (2005), Sargent et al. (2006) and Sicilia-Aguilar et al. (2007) we fitted observational and theoretical profiles of the silicate feature. The best model was chosen by minimizing the χ^2 criterion. In all cases, the observational continuum is fitted by a straight line in the interval $8 - 12 \mu\text{m}$. This simplest method does not contain nonphysical assumptions and works rather well in the narrow wavelength interval (Juhász et al., 2008). The calculations were made for layered spheres with $r_{\text{s,compact}} = 0.1 \mu\text{m}$ consisting of Be1 and MgFeSiO_4 .

The estimated porosity and amount of carbon in grains producing the silicate emission feature in protoplanetary discs are collected in online Table 1. At this stage, the stars with very pronounced crystalline peaks were eliminated from the consideration. Table 1 includes 47 stars (30 T Tau and 17 HAeBe stars). The obtained values of \mathcal{P} , $V_{\text{Be1}}/V_{\text{solid}}$, the ratio of masses of carbon to silicate $M_{\text{Be1}}/M_{\text{MgFeSiO}_4}$ and stellar age (if known) are given. Note that the determination of the age is often quite uncertain for pre-main-sequence stars (see discussion in Blondel & Tjin A Dje, 2006). Therefore, we do not discuss possible correlations.

The grain porosity exceeds 0.5 and the average value of \mathcal{P} is equal to $\langle \mathcal{P} \rangle = 0.82 \pm 0.12$. Such particles resemble aggre-

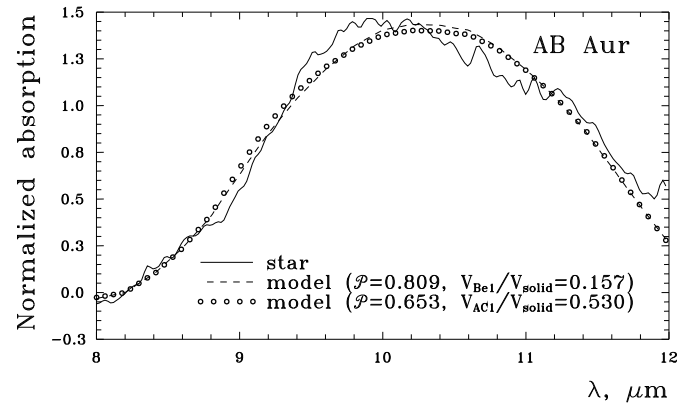


Fig. 4. The observational normalized profile of the $10 \mu\text{m}$ feature for the Herbig Ae/Be star AB Aur (van Boekel et al., 2005). The best fit profiles are shown for particles containing amorphous carbon in the form Be1 (dashed line) and AC1 (circles). The values of particle porosity \mathcal{P} and fractional amount of carbon $V_{\text{Be1}}/V_{\text{solid}}$ are indicated.

gates obtained both experimentally (Kempf et al., 1999) and theoretically (Shen et al., 2008)².

The amount of carbon in grains is not very large (average volume fraction $\langle V_{\text{Be1}}/V_{\text{solid}} \rangle = 0.202 \pm 0.085$ and average mass ratio $\langle M_{\text{Be1}}/M_{\text{MgFeSiO}_4} \rangle = 0.151 \pm 0.085$). These values increase by a factor of 3 – 4 if we replace Be1 by the less absorbing amorphous carbon AC1. This fact is illustrated in Fig. 4 where the results are given for both particle materials. Note that the particles containing AC1 are less porous.

The variation of grain porosity without significant change of grain mass may explain the behaviour of silicate emission. This explanation is an alternative to the commonly used idea of large grains in protoplanetary discs. To decide between the two hypotheses will be possible after spectropolarimetry in the $10 \mu\text{m}$ feature because a noticeable albedo of large grains manifests itself in polarization of scattered light. In this case we expect an unusual behaviour of polarization parameters (especially positional angle) within the feature profile in comparison with calculated profiles for dichroic extinction (see, e.g., Henning & Stognienko, 1993; Prokopenko & Il'in, 2007).

4. Crystalline silicates in composite grains

Another interesting problem is the degree of crystallinity of dust in protoplanetary discs which is related to the processes of partial grain evaporation and annealing (e.g., Gail, 2004). Due to the conversion of amorphous silicates to crystalline minerals, the particles may consist of different types of silicates. In order to show the effect of amorphous silicate matrix and vacuum on resonances produced by crystalline silicates we calculated the feature profiles for composite particles containing Mg-rich crystalline olivine $\text{Mg}_{1.9}\text{Fe}_{0.1}\text{SiO}_4$ as a component. The results are plotted in Fig. 5 where the upper panel illustrates the influence of particle porosity on position and strength of emission peaks. It is seen that variations of spectra are significant: the shape of the feature changes (cf. Fig. 2), some peaks totally disappear and new peaks arise. A very pronounced peak with a

² See also discussion in Li et al. (2003)

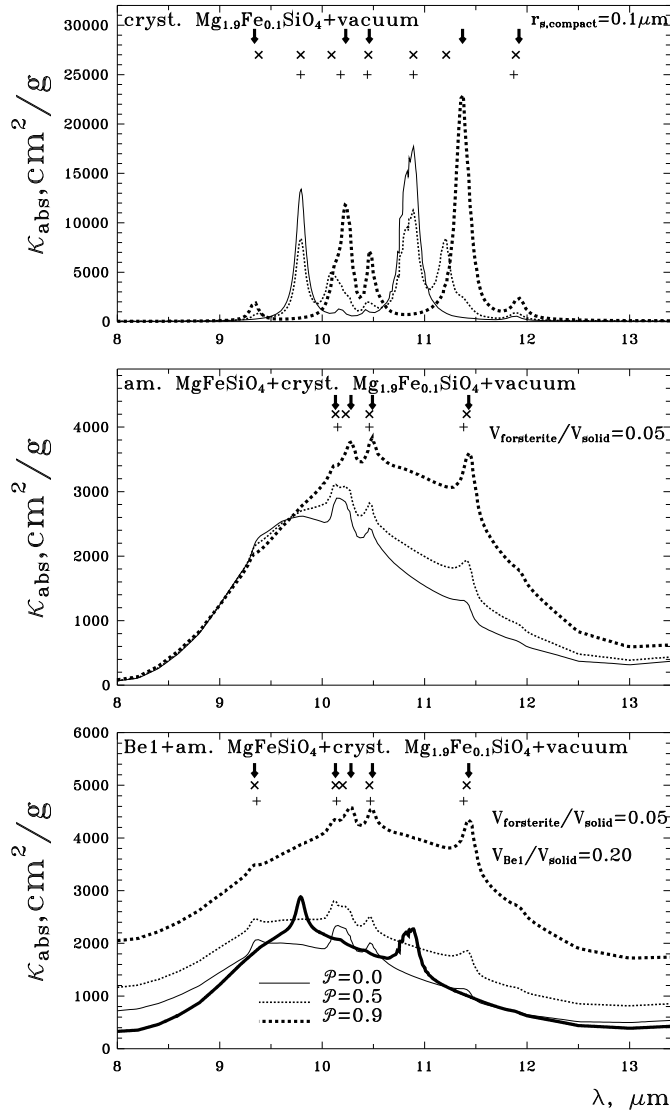


Fig. 5. Wavelength dependence of the mass absorption coefficient for compact and layered spheres with $r_{s,compact} = 0.1 \mu\text{m}$. The particles consist of crystalline olivine and vacuum (upper panel), amorphous silicate, crystalline olivine and vacuum (middle panel) and amorphous carbon, amorphous silicate, crystalline olivine and vacuum (lower panel). The volume fraction of crystalline olivine and Be1 is indicated. The solid curves correspond to compact particles. The position of peaks is marked. The thick solid line at the lower panel shows the mass absorption coefficient for the mixture of compact grains (external mixing) with volume fractions of constituents corresponding to solid curve (internal mixing). The effect of variation of crystalline resonances with particle porosity and composition is illustrated.

maximum near $\lambda = 11.37 \mu\text{m}$ is observed for very porous particles whereas compact and medium-porous particles have resonances near $\lambda = 10.89 \mu\text{m}$. The inclusion of crystalline silicates in a composite particle containing amorphous silicate (middle panel) or amorphous silicate and carbon (lower panel) changes the picture. The resonance near $\lambda \approx 11.4 \mu\text{m}$ is clearly seen at the long-wavelength wing of the feature. Its position slightly

shifts if the porosity changes. Fabian et al. (2001) found that such a peak appeared in the spectra of strongly elongated particles. A double peaked structure around $\lambda = 10.25 \mu\text{m}$ arises as well. Such structure was not previously noticed in spectra of crystalline olivines (H. Mutschke, priv. commun., 2007). Note that as expected the mixture of separate constituents (amorphous silicate, carbon and crystalline silicate, thick line in lower panel) do not lead to the shift of peaks. Further calculations with different materials for wider wavelength range and detailed comparison with *Spitzer* observations (see Watson et al., 2007) can help to resolve the problem of grain crystallization in protoplanetary discs and answer the question if the crystals occur in “isolation” or as part of porous grains.

Acknowledgements. We thank R. van Boekel, A. Schegerer, B. Sargent, M. Honda and A. Sicilia-Aguilar for sending the observational data in tabular form, H. Mutschke, V. Il’in, R. van Boekel, A. Juhász and the anonymous referee for helpful comments and suggestions. The work was partly supported by grants NSH 8542.2006.2, RNP 2.1.1.2152 and RFBR 07-02-00831 of the Russian Federation.

References

- Bertout, C., Siess, L. & Cabrit, S. 2007, *A&A*, 473, L21
 Blondel, P.F.S., & Tjin A Djie, H.R.E. 2006, *A&A*, 456, 1045
 Bouwman, J., Henning, Th., Hillenbrand, L.A., et al. 2008, *ApJ*, in press ([arXiv:0802.3033])
 Bouwman, J., Meeus, G., de Koter, A., Hony, S., Dominik, C., & Waters, L.B.F.M. 2001, *A&A*, 375, 950
 Dominik, C., & Tielens, A.G.G.M. 1997, *ApJ*, 480, 647
 Dorschner, J., Begemann, B., Henning, Th., Jäger, C., & Mutschke, H. 1995, *A&A*, 300, 503
 Fabian, D., Henning, Th., Jäger, C., & Mutschke, H., Dorschner, J. & Wehrhan, O. 2001, *A&A*, 378, 228
 Gail, H.-P. 2004, *A&A*, 413, 571
 Güdel, M., Briggs, K.R., Arzner, K. et al. 2006, *A&A*, 468, 353
 Henning, Th. 2008, *ESA Publ.*, in press
 Henning, Th. & Stognienko, R. 1993, *A&A*, 280, 609
 Henning, Th. & Stognienko, R. 1996, *A&A*, 311, 291
 Honda, M., Katata, H., Okamoto, Y.K., et al. 2006, *ApJ*, 646, 1024
 Jones, A.P. 2004, In *Astrophysics of dust*, ed. A.N. Witt, G.C. Clayton & B.T. Draine, ASP Conf., 309, 347
 Juhász, A., Henning, Th., Bouwman, J., Dullemond, C.P., Pascucci, I., Apai, D. 2008, *ApJ*, in press
 Kempf, S., Pfalzner, S. & Henning, Th. 1999, *Icarus*, 141, 388
 Kessler-Silacci, J.E., Augereau, J.-C., Dullemond, C.P., et al. 2006, *ApJ*, 639, 275
 Laor, A., & Draine, B.T. 1993, *ApJ*, 402, 441
 Li, A., Lunine, J.I. & Bendo, G.J. 2003, *ApJ*, 598, L51
 Li, M., Zhao, G. & Li, A. 2004, *ApJ*, 613, L145
 Min, M., Dominik, C., Hovenier, J.W., de Koter, A. & Waters, L.B.F.M. 2006, *A&A*, 445, 1005
 Natta, A., Testi, L., Calvet, N., Henning, Th., Waters, R., & Wilner, D. 2007, In *Protostars and Planets V*, ed. B. Reipurth, D. Jewitt & K. Keil (University Arizona Press), 767
 Ormel, C.W., Spaans, M. & Tielens, A.G.G.M. 2007, *A&A*, 461, 215
 Prokopenko, M.S. & Il’in, V.B. 2007, *Astron. Lett.*, 33, 699
 Rouleau, F., & Martin, P.G. 1991, *ApJ*, 377, 526
 Sargent, B., Forrest, W.J., D’Alessio, P., et al. 2006, *ApJ*, 645, 395
 Schegerer, A., Wolf, S., Voshchinnikov, N.V., Przygodda, F., & Kessler-Silacci, J.E. 2006, *A&A*, 456, 535
 Shen, Y., Draine, B.T., & Johnson, E.T. 2008, *ApJ*, in press ([arXiv:0801.1996])

- Sicilia-Aguilar, A., Hartman, L.W., Watson, D., Bohac, C., Henning, Th., & Bouwman, J. 2007, *ApJ*, 659, 1637
- van Boekel, R., Min, M., Waters, L.B.F.M., et al. 2005, *A&A*, 437, 189
- Voshchinnikov, N.V., & Mathis, J.S. 1999, *ApJ*, 526, 257
- Voshchinnikov, N.V., Il'in, V.B., & Henning, Th. 2005, *A&A*, 429, 371
- Voshchinnikov, N.V., Il'in, V.B., Henning, Th., & Dubkova, D.N. 2006, *A&A*, 445, 167
- Watson, D.M., Leisenring, J.M., Furlan, E., et al. 2007, *ApJS*, in press ([arXiv:0704.1518])

Table 1. Grain porosity and fractional amount of carbon in grains as derived from fitting the 10 μm silicate emission feature.

Star	Type ¹	\mathcal{P}	$V_{\text{BeI}}/V_{\text{solid}}$	$M_{\text{BeI}}/M_{\text{MgFeSiO}_4}$	Age, Myr	Ref. ²	Comment
Tr 37 73-758	t	0.906	0.214	0.153	1.8	1	
Tr 37 11-2146	t	0.886	0.182	0.125	0.9	1	
Tr 37 11-2037	t	0.850	0.192	0.133	2.5	1	
Tr 37 11-2031	t	0.786	0.146	0.096	2.5	1	
Tr 37 14-183	t	0.792	0.303	0.243	0.9	1	
Tr 37 82-272	t	0.845	0.186	0.128	10.5	1	
Tr 37 12-2113	t	0.778	0.159	0.106	1.1	1	
Tr 37 13-157	t	0.842	0.232	0.170	2.4	1	
Tr 37 91-155	t	0.966	0.211	0.150	1.7	1	
Tr 37 54-1547	t	0.639	0.134	0.087	5.7	1	
Tr 37 13-1250	t	0.759	0.109	0.069	3.3	1	
Tr 37 23-162	t	0.810	0.229	0.166	6.6	1	
Tr 37 01-580	t	0.626	0.159	0.106	8.7	1	
NGC 7160 DG-481	h	0.882	0.338	0.286	12.0	1	
SU Aur	t	0.850	0.105	0.066	3.9	2	age from (5)
GW Ori	t	0.802	0.081	0.049	1.0	2	
CR Cha	t	0.856	0.076	0.046	1.0	2	
Glass I	t	0.858	0.175	0.119	1.0	2	
WW Cha	t	0.961	0.152	0.101	0.3	2	
SZ 82	t	0.940	0.240	0.177	1.1	2	
AS 205S	t	0.862	0.207	0.146	0.1	2	
Haro 1-16	t	0.728	0.109	0.068	0.5	2	
AK Sco	t	0.589	0.107	0.067	7.6	2	age from (5)
FM Tau	t	0.882	0.168	0.113	2.8	3	age from (6)
GG Tau A	t	0.621	0.263	0.200	3.3	3	age from (7)
GG Tau B	t	0.941	0.335	0.282	1.6	3	age from (7)
GM Aur	t	0.789	0.142	0.093	7.4	3	age from (7)
IP Tau	t	0.672	0.181	0.124	4.3	3	age from (7)
TW Hya	t	0.944	0.115	0.073	10.0	3	age from (2)
Hen 3-600 A	t	0.990	0.195	0.136		3	
V410 Anon 13	t	0.852	0.338	0.286		3	
HD 104237	h	0.878	0.267	0.204	4.8	4	age from (5)
HD 142527	h	0.831	0.304	0.244	1.0	4	
HD 142666	h	0.911	0.222	0.160	4.4	4	age from (5)
HD 144432	h	0.681	0.111	0.070	6.65	4	age from (5)
HD 144668	h	0.942	0.429	0.422	0.5	4	
HD 150193	h	0.711	0.157	0.104	2.6	4	age from (5)
HD 163296	h	0.760	0.185	0.127	6.0	4	age from (5)
HD 179218	h	0.983	0.235	0.172	1.3	4	
HD 245185	h	0.899	0.109	0.068	3.3	4	age from (5)
HD 36112	h	0.469	0.120	0.076	4.4	4	age from (5)
HD 37357	h	0.731	0.181	0.124	10.0	4	
HD 37806	h	0.935	0.357	0.311	0.8	4	
AB Aur	h	0.809	0.157	0.105	4.8	4	age from (7)
HK Ori	h	0.824	0.346	0.296	5.8	4	age from (5)
UX Ori	h	0.538	0.146	0.096	2.8	4	age from (5)
V380 Ori	h	0.964	0.388	0.355	7.4	4	age from (5)

¹Meaning of symbols: t = T Tau star, h = Herbig Ae/Be star.²References for observational data: (1) Sicilia-Aguilar et al. (2007); (2) Schegerer et al. (2006); (3) Sargent et al. (2006); (4) van Boekel et al. (2005); (5) Blondel & Tjin A Djie (2006); (6) Güdel et al. (2007); (7) Bertout et al. (2007).